Deposition of Hydrocarbon Films by Means of Helium-Ethylene Fed Glow Dielectric Barrier Discharges

Fiorenza Fanelli,* Francesco Fracassi, Riccardo d'Agostino

Dipartimento di Chimica, Università degli Studi di Bari–IMIP CNR, via Orabona 4, 70126 Bari, Italy
Fax: +39 0805443405; E-mail: fiorenzafanelli@chimica.uniba.it

Keywords

Atmospheric pressure, ethylene, glow dielectric barrier discharge (GDBD), plasma enhanced chemical vapour deposition (PE-CVD)

Summary

The present work provides a detailed study of helium-ethylene dielectric barrier glow discharges. The effect of ethylene concentration, total gas flow rate, excitation frequency and applied voltage has been investigated in order to clarify both discharge operational mode and coating composition. The discharge has been characterized by means of electrical measurements and optical emission spectroscopy, while the stable species contained in the gas effluent have been sampled and analyzed using gas chromatography with mass spectrometry detection to achieve indications on the reactive fragments generated inside the discharge. It has been observed that a polyethylene-like coatings can be obtained with deposition rates ranging between 20 and 80 $nm \cdot min^{-1}$ in a wide range of electrical conditions.

Introduction

Dielectric barrier discharges (DBDs) have received increased attention in recent years, since the advantage of atmospheric operation coupled with the non-equilibrium conditions makes these approaches a promising alternative to the low pressure counterpart for surface processing of materials.[1]

It is well-known that DBDs very often operate in a filamentary regime (FDBD); however, under particular experimental conditions, a homogeneous regime, the so-called glow dielectric barrier discharge (GDBD), can be obtained.[2-7] A lot of work has been done to investigate these two discharge regimes and the transition between FDBD and GDBD in helium and nitrogen. In the field of materials processing the debate on this topic resulted into two main research currents: the first proposes the utilization of the filamentary discharges, in spite of the intrinsic inhomogeneity, for their easy operation; the second prefers the glow regime that should be more suitable for uniform surface treatment. The atmospheric pressure glow discharge (APGD), in fact, attracts significant research interest for its technological potential, even though, due to the quite restrictive conditions under which homogeneity can be obtained, the operational window is quite narrow and an adequate process control is not available so far. Particular attention should be paid to study the influence of different process parameters on the discharge characteristics and to the fact that the addition of reactive compounds to the feed gas, as it is required in deposition processes, can drastically affect discharge stability and behaviour. Unfortunately, to our knowledge, a complex and exhaustive study on this theme has not been published up to now; therefore, we present a detailed exploration of helium-ethylene fed DBDs in the glow regime in this article.

Low pressure plasma enhanced chemical vapour deposition (PECVD) of hydrogenated amorphous carbon (a-C:H) thin films has been widely studied utilizing several monomers. Polymeric coatings with well-defined characteristics, such as hydrogen concentration and Csp^3/Csp^2 ratio, have been deposited.[8-14] Interesting results have been reported since the 70's; for instance in 1974, Kobayashi

et al.,[15, 16] in ethylene fed plasmas, obtained a polymer-like coating with a strong tendency to oxidise after preparation. Even at low pressure, powder formation was observed. The results were exploited to investigate the hypothesis of free-radical polymerisation that mainly occurs in the gas phase. Yasuda et al.[17-19] widely investigated the effects of different process parameters and of the reactor design on low pressure plasma assisted deposition of polyethylene. They observed that, as a consequence of its reactivity, ethylene deposited uniformly over wide areas of the reactor and produced a highly branched and saturated hydrocarbon coating, which slowly oxidized with storage.

One of the first investigations of atmospheric pressure deposition in hydrocarbon containing discharges was published in 1979 by Donohoe and Wydeven,[20] namely the polymerisation of ethylene diluted in helium, in an uniform atmospheric pressure pulsed discharge. In this pioneering work a soft polymeric film with a low cross-linking degree was obtained; nevertheless, a complete investigation of chemical structure of the coating was not performed. The polymerisation was explained by a free-radical chain reaction scheme initiated by electron collisions. The study of high molecular weight oligomers in the gas phase allowed the investigation of powder formation phenomena. The polymerisation of ethylene in helium-containing atmospheric pressure glow discharges has also been reported by Yokoyama et al..[21] The effect of ethylene concentration and discharge current was studied; an increase of the deposition rate up to 1 $\mu m \cdot h^{-1}$ was observed as a function of the rising discharge current. A polyethylene-like film, similar to those deposited with low pressure PE-CVD, was obtained but unfortunately no results on the chemical characteristics of the film nor any indication on its oxygen content were reported.

Many other studies concerning hydrocarbon deposition in DBD from several monomers and gas mixtures, frequently in a filamentary regime, have been reported in the scientific literature.[22-30] In particular, Goossens et al.[24, 25] studied ethylene deposition in mixtures with helium or argon. In both cases the characteristics of a polyethylene-like coating were observed but, compared to He plasma, Ar plasma gave a clear and more solid polymer with good adhesion to all substrates. A

deposition rate of about 100 nm·min^{-1} was obtained by employing 1 slm of reactive gas mixed with 10 slm of inert gas.[25] The presence of bonded oxygen was observed in the polymer, probably originated from atmospheric exposure.[24] Recently, Girard-Lauriault et al.[27] reported a novel material, nitrogen-rich plasma-polymerized ethylene (PPE:N), which was deposited using atmospheric pressure dielectric barrier discharges fed by means of nitrogen (ca. 10 slm) and ethylene (ca. 10sccm). The nitrogen content in the film were readily and reproducibly controlled by varying C_2H_4 concentration in the feed gas.

In the present work, results on the deposition of a-C:H thin films in Glow DBD fed with helium-ethylene are presented. The operational range of the glow regime as a function of input power, ethylene concentration, and residence time has been investigated by performing electrical characterization of the discharge. The chemical characteristics of the coatings as well as their water contact angles are reported over the experimental range investigated.

Experimental Methodology

The experimental apparatus is shown schematically in figure 1. It consists of a parallel plate electrode system (5 mm interelectrode gap) contained in a Plexiglas box (~ 60 l volume); each square electrode (9 cm^2 area) is covered by a 0.6 mm thick Al_2O_3 plate (CoorsTek, 96% purity). The plasma is generated by means of an AC high voltage (HV) power supply, composed of a variable frequency generator (TTi TG215), a linear amplifier (Outline PA4006) and a high voltage transformer (Montoux). The excitation frequency (*f*) can be varied in the range 0.5 – 30 kHz, and the applied voltage can be raised up to 10 kV_{rms}.

The discharge was fed with He-C_2H_4 mixtures (Air Liquide, Helium C, Ethylene N35) and the gas flow rates were controlled by MKS electronic mass flow controllers. The feed gas was introduced in the interelectrode zone through an inlet slit and pumped with a rotary pump through an outlet slit positioned on the opposite side. Before each experiment the Plexiglas chamber was flushed with a

high flow rate of helium (5 slm) for 40 min. The purge time was fixed at 40 min at the beginning of the present study and it was not optimized during the progress of the work.

The electrical characterization of the discharge was performed with a digital oscilloscope (Tektronix TDS2014); the voltage applied to the electrodes (V_a) was measured by means of a high voltage probe (Tektronix, P6015) and the discharge current (I_m) was evaluated by measuring the voltage drop across a 50 Ω resistor connected in series with the ground electrode.

Optical emission spectroscopy was perfomed by collecting the UV-VIS spectra (200 – 900 nm) through an optical fiber using an Optical Multichannel Analyser (OMA). The radiation emitted by the plasma was guided by a 1 m quartz fiber to a monochromator (0.300 m focal length imaging monochromator, ACTON SP-300i) equipped with a 1200 g/mm grating, and by a CCD detector (SpectruMM^{TM} 100B, Princeton Instruments).

A stainless steel liquid nitrogen trap, located between the reactor and the rotary pump, allowed us to sample the stable species contained in the exhaust gas. The sampling was performed for three hours, then the trap was isolated from the system, the condensate was dissolved in nonane (Aldrich, 99 % purity) and analysed by means of gas chromatography (GC) with mass spectrometric (MS) detection. The GC apparatus (GC 8000^{Top} Thermoquest Corporation) was equipped with an J&B DB-1 capillary column (polydimethylsiloxane 0.25 μm thick stationary phase, length of 30 m, i.d. of 0.25 mm). The analyses were performed with 1 sccm of He as carrier gas, at 200°C injector temperature and column temperature programmed from 22 to 200°C (6 min at 22 °C, linear heating rate of 10°C·min^{-1}, 1 min at 200°C). Separated products were analysed with a quadrupole mass spectrometer (Voyager, Finnigan, Thermoquest Corporation), at the interface and source temperature of 250 and 200 °C, respectively. Mass spectra were recorded in the *m/z* range 15 – 500 u.m.a. at the standard ionizing electron energy of 70 eV. The products were identified by means of available libraries.[31]

The chemical characterization of the deposited films was carried out by means of X-ray photoelectron spectroscopy (XPS) and Fourier transform infrared spectroscopy (FT-IR). XPS was

performed with a PHI ESCA 5300 (non-monochromatic Mg K_α radiation) on coatings deposited on glass substrates, while for FT-IR analysis (Bruker Equinox 55 spectrometer) the coatings were deposited on CaF_2 substrates.

Static water contact angle (WCA) measurements were carried out by means of a Ramé-Hart manual goniometer (model A-100) using the sessile drop technique (double distilled water droplet of 2 μl), with an uncertainty of ± 3°.

Film thickness was evaluated on substrates partially masked during the deposition using an Alpha-Step® 500 KLA Tencor Surface profilometer, at different positions inside the interelectrode gap, i.e. as a function of the gas residence time. In order to compare the results obtained under different experimental conditions, the average value of the deposition rate was considered in the region 10 - 20 mm from the gas entrance inside the discharge area; at each experimental point an error bar corresponding to the minimum and the maximum values of the measured deposition rate was associated. Scanning electron microscopy was utilized for morphological characterization.

The experimental conditions utilized for the study are listed in table 1.

Results and Discussion

The electrical characterization of the discharge showed that microdischarges appear for excitation frequencies lower than 9 kHz, whatever the concentration of ethylene in helium; if the frequency is higher than 10 kHz, a periodical discharge current signal can be observed for up to 0.5 % of ethylene in the feed gas. The current signal is periodical with the same period of the applied voltage and usually comprises only one peak per half cycle, as for a typical current signal of a GDBD in helium.[4] The higher the ethylene concentration, the higher the breakdown voltage and the discharge current amplitude.

Moreover, the discharge current consists of only one peak per half-cycle if the applied voltage is lower than 3.4 kV_{p-p}, while for higher voltages secondary current peaks are observed in addition to the principal one (figure 2). The periodicity of the current signal and the individual current pulse

duration suggest that the discharge is homogeneous even though it operates with successive breakdowns during a single half cycle. These multiple current pulses are usually produced when the applied voltage exceeds the breakdown voltage.[32-34]

As expected (figure 3), due to the particular gas injection system, the thickness of the deposit increases with the distance from the gas admission point inside the discharge area (i.e. residence time of the gas). The deposition rate increases by increasing the ethylene concentration in the feed gas from 22 to 40 $nm \cdot min^{-1}$ on the average, for ethylene concentration of 0.1 and 0.5 %, respectively. Figure 4 shows the normalised FTIR absorption spectra of deposits as a function of ethylene concentration. The main spectral features are the broad band between 3000 and 2800 cm^{-1} due to CH stretching vibration modes and the two signals between 1480 and 1370 cm^{-1} from CH_2 and CH_3 bending. No appreciable olefinic CH signal can be observed. The intensity and structure of the CH stretching band could be consistent with an amorphous and polymer-like structure with mainly sp^3 carbon bonded to hydrogen.[13, 35-39] Some oxygen is also contained in the coating in the forms of OH (3450 cm^{-1}), C=O (1720 cm^{-1}) and C-O (1090 cm^{-1}) groups.[36, 38, 39] As the ethylene concentration increases, the C=O band disappears, and the OH and C-O signals become less pronounced. These functionalities are due to O_2 and H_2O contaminations in the deposition chamber and/or to oxidation of residual free radicals after atmospheric exposure.

In agreement with FT-IR, XPS analyses show a decrease of the oxygen uptake, from 8 to 0.8 %, as the ethylene concentration in the feed passes from 0.1 to 0.5 %, at the same time as WCA varies from 75 to 90°.

In order to investigate stability of the coatings, the deposits obtained at 0.5 % of C_2H_4, 20 kHz and 2.8 kV_{p-p} were also analyzed after one month of aging in air. Only a slight increase of the OH and C-O bands was detected with FT-IR compared with the as deposited films (figure 5), and the oxygen uptake, evaluated by means of XPS, passed from 0.8 % on as deposited film to 2.5 % after 1 month following deposition.

By increasing the total gas flow rate at ethylene concentration of 0.5 % in the feed (i.e. by reducing the gas residence time), the average deposition rate decreased slightly from 40 to 35 nm·min^{-1} and a less pronounced film thickness variation with position in the discharge area was detected. On the other hand, FTIR showed a less pronounced OH and C-O absorption bands while an oxygen concentration lower than 1.5 % was detected by means of XPS analyses.

In order to investigate the effect of input power, the frequency and the voltage of the discharge were varied separately. By increasing the frequency, i.e. the number of current pulses per unit of time, a growth of the discharge power and of the average deposition rate from 20 up to 80 nm·min^{-1} was detected while, by increasing the voltage at fixed excitation frequency, i.e. the energy per half cycle, an approximately linear growth of the power density and a less pronounced increase of the average deposition rate from 40 to 50 nm·min^{-1} were observed. The FTIR spectra were not appreciably affected by frequency and voltage variation, while XPS analyses showed that oxygen concentration was always lower than 3 % under all the experimental conditions explored.

The quality of the coating, evaluated with SEM was always good, in particular no evidence of powders or defects were found (figure 6).

The main emission spectroscopic features in He and He-C_2H_4 plasmas are listed in Table 2. Helium GDBD was characterized by intense emissions from helium and certain impurities, i.e. nitrogen, oxygen and water.[40, 41] Among contaminants, the emission of N_2^+ at 391 nm, generated by Penning ionisation directly in the excited state[4], was the most intense. Ethylene addition to the feed gas caused a reduction of all the emission intensities and in particular of those of oxygen-containing species which completely disappear, while CH (4300 Å system) and C_2 (Swan system) emissions were detected.

A typical chromatogram of exhaust gas sampled with the cold trap is shown in figure 7. The concentration of by-products in the exhaust was always very low and it was not affected by the experimental conditions. Only butane was present in appreciable quantities corresponding to 0.01

sccm at 0.5 % of C_2H_4, 20 kHz and 2.8 kV_{p-p}; the other saturated and unsaturated hydrocarbons identified with mass spectrometry were present in very low amounts (< 0.001 sccm).

Conclusion

The results presented here show that it is possible to deposit thin hydrocarbon films over a wide range of glow dielectric barrier discharge conditions using helium-ethylene containing feed. The observed oxygen uptake can be ascribed to contaminations in the deposition chamber and/or to post-deposition reactions with atmospheric oxygen or water. The chemical characteristics of the coatings, their oxygen content in particular, depend on the ethylene concentration in the feed gas as well as on the total gas flow rate. (i.e. gas residence time).

The disappearance of oxygenated species emissions in the spectra of ethylene-containing GDBD could be due to the well known high reactivity of hydrocarbons with oxygenated species, such as OH radicals.[42, 43] Reactions of ethylene and other hydrocarbon fragments with oxygen-containing species could lead to the formation of volatile non polymerizing species and/or oxygenated film precursors, in part responsible of the oxygen uptake of the coatings.

Regarding the mechanism of film formation, it is reasonable to assume that the contribution of gas phase reaction to the polymerization process is quite low and that gas-surface reactions play the major role in the polymerization process. Two pieces of evidence support this assumption, namely the fact that only butane and no other recombination products of ethylene fragmentation were detected in appreciable quantities by means of GC-MS in the exhaust, and the absence of powders, which were never detected by SEM. If homogeneous gas phase reactions were also important in the polymerization process not only butane formation but more complex oligomers and powder should have been detected.

Acknowledgements

Dr. Françoise Massines and Dr. Nicolas Gherardi (Laboratoire de Génie Electrique de Toulouse,

Université Paul Sabatier, Toulouse, France) are gratefully acknowledged for scientific support in assembling of the experimental set-up.

References

[1] U. Kogelschatz, *Plasma Chem. Plasma Proc.* **2003,** *23*, 1

[2] T. Yokoyama, M. Kogoma, T. Moriwaki, S. Okazaki, *J. Phys. D: Appl. Phys.* **1990**, *23*, 1125.

[3] S. Okazaki, M. Kogoma, M. Uehara, Y. Kimura, *J. Phys. D: Appl. Phys.* **1993**, 26, 889.

[4] F. Massines, G. Gouda, *J. Phys. D : Appl. Phys.* **1998**, *31*, 3411.

[5] F. Massines, A. Rabehi, P. Decomps, R. Ben Gadri, P. Segur, C. Mayoux, *J. Appl. Phys.* **1998**, *83*, 2950.

[6] N. Gherardi, G. Gouda, E. Gat, A. Ricard, F. Massines, *Plasma Sources Sci. Technol.* **2000**, 9, 340.

[7] F. Massines, P. Segur, N. Gherardi, C. Khamphan, A. Ricard, *Surf. Coat. Technol.* **2003**, *174 – 175*, 8.

[8] P. Courdec and Y. Catherine, *Thin Solid Films* **1987**, *146*, 93.

[9] N. Mutsukura, K. Miyatani, *Diam. Relat. Mater.* **1995**, *4*, 342.

[10] N. V. Novikov, M. A. Voronkin, S. N. Dub, I. N. Lupich, V. G. Malogolovets, B. A. Maslyuk, G. A. Podzayarey, *Diam. Relat. Mater* **1997**, *6*, 574.

[11] B. K. Kim and T. A. Grotjohn, *Diamond Relat. Mater.* **2000**, *9*, 37.

[12] J. Hong, A. Goullet and G. Turban, *Thin Solid Films*, **2000**, *364*, 144.

[13] J. Robertson, *Mat. Sci. .Engin.* **2002**, *R 37*, 129.

[14] D. Liu, S. Yu, Y. Liu, C. Ren, J. Zhang, T. Ma, *Thin Solid Films* **2002**, *414*, 163.

[15] M. Niinomi, H. Kobayashi, A. T. Bell, M. Shen, *J. Appl. Phys.* **1973,** *44*, 10.

[16] H. Kobayashi, A. T. Bell and M. Shen, *Macromol.* **1974**, *7*, 3.

[17] H. Yasuda, M. O. Bumgarner, H. C. Marsh and N. Morosoff, *J. Polym. Sci. Polym. Chem. Ed.* **1976**, *14*, 195.

[18] H. Yasuda and T. Hirotsu, *J. Polym. Sci. Polym. Chem. Ed.* **1978**, *16*, 219.

[19] H. Yasuda and T. Hirotsu, *J. Polym. Sci. Polym. Chem. Ed.* **1978**, *16*, 313.

[20] K. G. Donohoe, T. Whydeven, *J. Appl. Polym. Sci.* **1979**, *23*, 2591.

[21] T. Yokoyama, M. Kogoma, S. Kanazawa, T. Moriwaki, S. Okazaki, *J. Phys. D: Appl. Phys*. **1990**, *23(3)*, 374.

[22] S. P. Bugaev, A. D. Korotaev, K. V. Oskomov and N. S. Sochugov, *Surf. Coat. Technol.* **1997**, *96*, 123.

[23] R. Thyen, A. Weber, C.-P. Klages, *Surf. Coat. Technol.* **1997**, *97*, 426.

[24] O. Goossens, E. Dekempeneer, D. Vangeneugden, R. Van de Leest, C. Leys, *Surf. Coat. Technol.* **2001**, *142-144*, 474.

[25] O. Goossens, S. Paulassens, D. Vangeneugden, H. Vrielinck, F. Callens, C. Leys and J. Meneve, *New Diamond Frontier Carbon Technol.* **2003**, *13(4)*, 221.

[26] S. Paulussen, R. Rego, O. Goossens, D. Vangeneugden and K. Rose, *J. Phys. D: Appl. Phys* **2005**, *38*, 568.

[27] P.-L. Girard-Lauriault, F. Mwale, M. Iordanova, C. Demers, P. Desjardins and M. R. Wertheimer, *Plasma Process. Polym.* **2005**, *2*, 263.

[28] K. K. Mishra, R. K. Khardekar, R. Dingh and H. C. Pant, *Rev. Scient. Instr.* **2002**, *73*, 9.

[29] C.-P. Klages, M. Eichler and R. Thyen, *New Diam. Front. Carb. Technol.* **2003**, *13*, 4.

[30] D. Liu, G. Benstetter, Y. Liu, X. Yang, S. Yu and T. Ma, *New Diam. Front. Carb. Technol.* **2003**, *13*, 4.

[31] NIST and Wiley libraries in *MassLab Release 1.4 (GC/MS Data System Software Finngan).*

[32] T. Nozaki, Y. Miyazaki, Y. Unno and K. Okazaki, *J. Phys. D: Appl. Phys*. **2001**, *34*, 3383.

[33] I. Radu, R. Bartnikas, G. Czeremuszkin and M. R. Wertheimer, *IEEE Trans. Plasma Sci.* **2003**, *31*, 1363

[34] I. Radu, R. Bartnikas and M. R. Wertheimer, *J. Phys. D: Appl. Phys.* **2005**, *38*, 539

[35] B. Dischler, A. Bubenzer and P. Koidl, *Solid State Communications* **1983**, *48*, 2.

[36] J. Rinstein, R. F. Stief, L. Ley and W. Beyer, *J. Appl. Phys.* **1998**, *84*, 7.

[37] J. E. Bourée, C. Godet, R. Etemadi, B. Drévillon, *Synthetic Materials* **1996**, *76*, 191.

[38] I. Retzko, J. F. Friedrich, A. Lippitz, W. E. S. Unger, *J. Elect. Spectro. Relat. Phenom.* **2001** *121*, 111.

[39] V. Kulikovsky, V. Vorlicek, P. Bohac, A. Kurdyumov and L. Jastrabik, *Thin Solid Films* **2004**, *447-448*, 223.

[40] A. R. Striganov and N. S. Sventiskii, *Tables of Spectral Lines of Neutral and Ionized Atoms*, IFI/Plenum, New York - Washington, 1968.

[41] R. W. B. Pearse and A. G. Gaydon, *The Identification of Molecular Spectra*, 4th ed., Chapman and Hall, London, 1976.

[42] D. D. Davis, S. Fischer, R. Schiff, R. T. Watson and W. Bollinger, *J. Chem. Phys.* **1975**, *63*, 5.

[43] C. J- Howard, *J. Chem. Phys.* **1976**, *65*, 11.

Figure captions

Figure 1. Schematic of the experimental apparatus.

Figure 2. Voltage and measured current at f = 20 kHz, [C_2H_4] = 0.5 % : (a) V_a = 2.8 kV_{p-p}; (b) 4.0 kV_{p-p}.

Figure 3. Schematic of the electrode system and typical deposition rate profile as a function of the position in the discharge area (f = 20 kHz, V_a = 2.8 kV_{p-p}, ϕ_{He} = 2slm, $\phi_{C_2H_4}$ = 10 sccm, [C_2H_4] = 0.5 %).

Figure 4. Normalized FTIR spectra of films deposited as a function of ethylene concentrations in the feed (f = 20 kHz, V_a = 2.8 kV_{p-p}, [C_2H_4] = 0.1- 0.5 %).

Figure 5. FTIR spectra of film as deposited and after one month ageing in air (f = 20 kHz, V_a = 2.8 kV_{p-p}, [C_2H_4] = 0.5 %, ϕ_{He} = 2slm, $\phi_{C_2H_4}$ = 10 sccm).

Figure 6. SEM images of the deposited film at different values of the excitation frequency: (a) 10 kHz, (b) 20 kHz, (c) 30 kHz.

Figure 7. Typical gas-chromatogram of exhaust (f = 20 kHz, V_a = 2.8 kV_{p-p}, [C_2H_4] = 0.5 %, ϕ_{He} = 2slm, $\phi_{C_2H_4}$ = 10 sccm, sampling time = 3h).

Table 1. Process parameters for GDBD in helium-ethylene mixtures.

f (kHz)	V_a (kV_{p-p})	P ($W \cdot cm^{-2}$)	ϕ_{He} (slm)	$\phi_{C_2H_4}$ (sccm)	$[C_2H_4]$ (%)
20	2.8	0.30	2	2 –10	0.1 – 0.5
20	2.8	0.30	2 – 5	10 – 25	0.5
10 - 30	2.8	0.14 – 0.49	2	10	0.5
20	2.8 – 4.0	0.30 – 0.42	2	10	0.5

Table 2. Emitting species in helium and helium-ethylene GDBD[40, 41].

Emitting specie	Observed transition	He GDBD	He/C_2H_4 GDBD
He	2s ^{3}S – 3p ^{3}P°, 3888 Å	✔	✔
	2p ^{3}P° – 3d ^{3}D, 4472 Å	✔	✔
	2p ^{1}P° – 4d ^{1}D, 4922 Å	✔	✔
	2s ^{1}S – 3p ^{1}P°, 5016 Å	✔	✔
	2p ^{3}P° – 3d ^{3}D, 5875 Å	✔	✔
	2p ^{1}P° – 3d ^{1}D, 6678 Å	✔	✔
	2p ^{3}P° – 3d ^{1}D, 7067Å	✔	✔
	2p ^{1}P° – 3s ^{1}S, 7281Å	✔	✔
H	H_β, 4861 Å	✔	✔
	H_α, 6562 Å	✔	✔
O	3p ^{5}P – 5d ^{5}D°, 5329 Å	✔	
	3p ^{5}P – 6s ^{5}S°, 5435 Å	✔	
	3p ^{3}P – 6s ^{3}S°, 6046 Å	✔	
	3p ^{5}P – 4d ^{5}D°, 6158 Å	✔	
	3p ^{5}P – 5s ^{5}S°, 6454 Å	✔	
	3s ^{5}S° – 3p ^{5}P, 7773 Å	✔	
	3s ^{3}S° – 3p ^{3}P, 8446 Å	✔	
N_2	$C^3\Pi_u$ – $B^3\Pi_g$ (Second positive system)	✔	✔
N_2^+	$B^2\Sigma_u^+$ – $X^2\Sigma_g^+$ (First negative system)	✔	✔
NO	$A^2\Sigma^+$ – $X^2\Pi$ (γ system)	✔	
O_2^+	$A^2\Pi_u$ - $X^2\Pi_g$ (Second negative system)	✔	
OH	$A^2\Sigma^+$ – $X^2\Pi$ (3064 Å system)	✔	
CH	$A^2\Delta$ – $X^2\Pi$ (4300 Å system)		✔
C_2	$A^3\Pi_g$ – $X'^3\Pi_u$ (Swan system)		✔

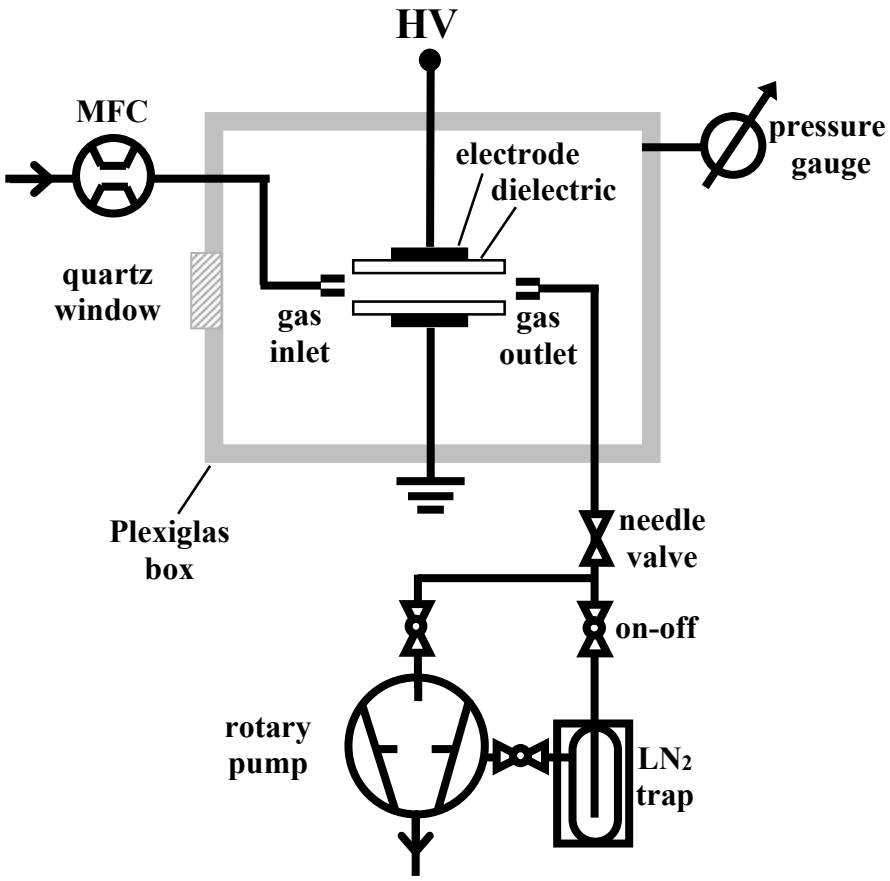
HV
MFC
pressure
gauge
electrode
dielectric
quartz
window
gas
inlet
gas
outlet
Plexiglas
box
needle
valve
on-off
rotary
pump
LN2
trap

Figure 1

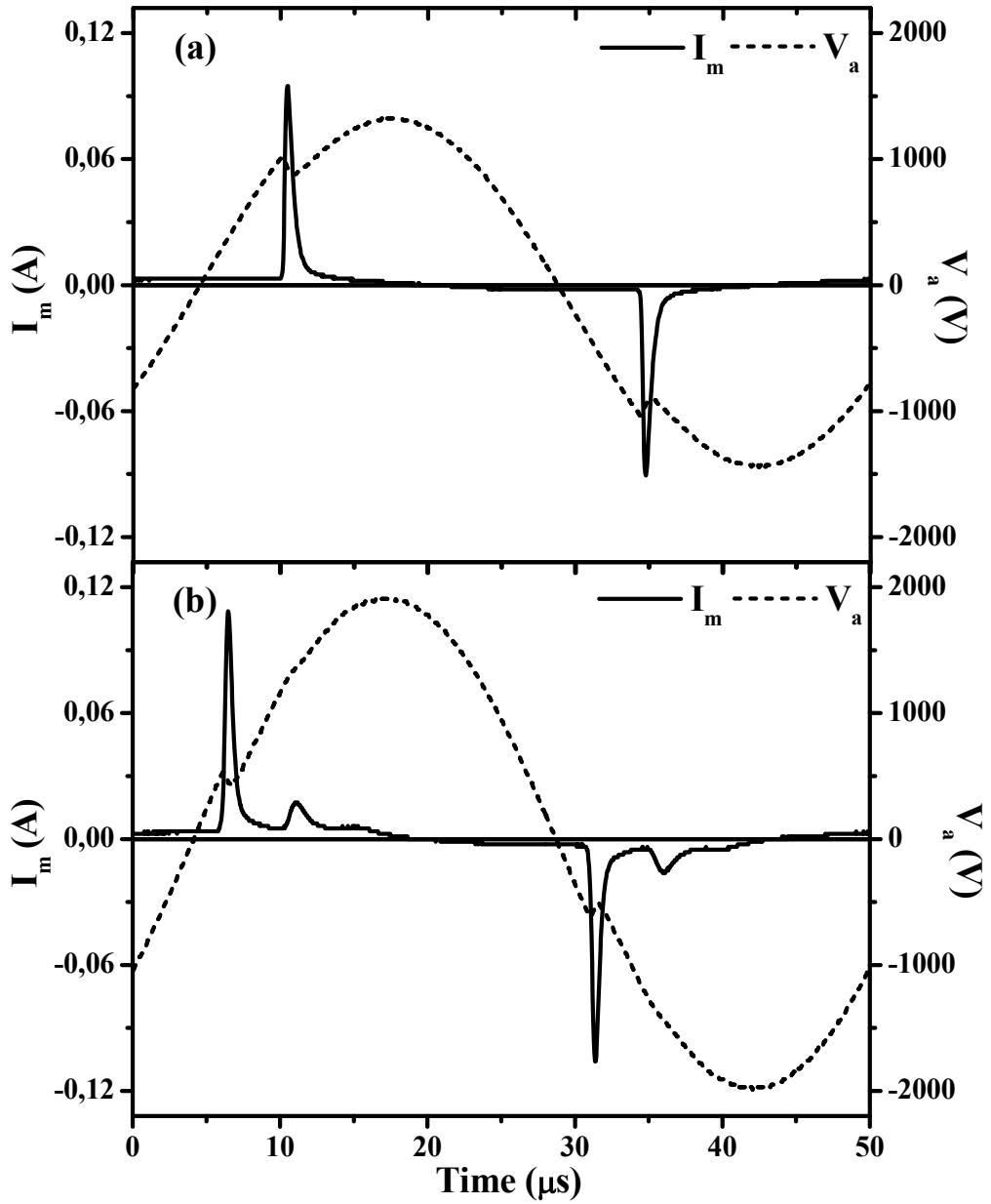
(a)
(b)
I_m
V_a
I_m (A)
V_a (V)
0,12
0,06
0,00
-0,06
-0,12
2000
1000
0
-1000
-2000
0
10
20
30
40
50
Time (μs)

Figure 2

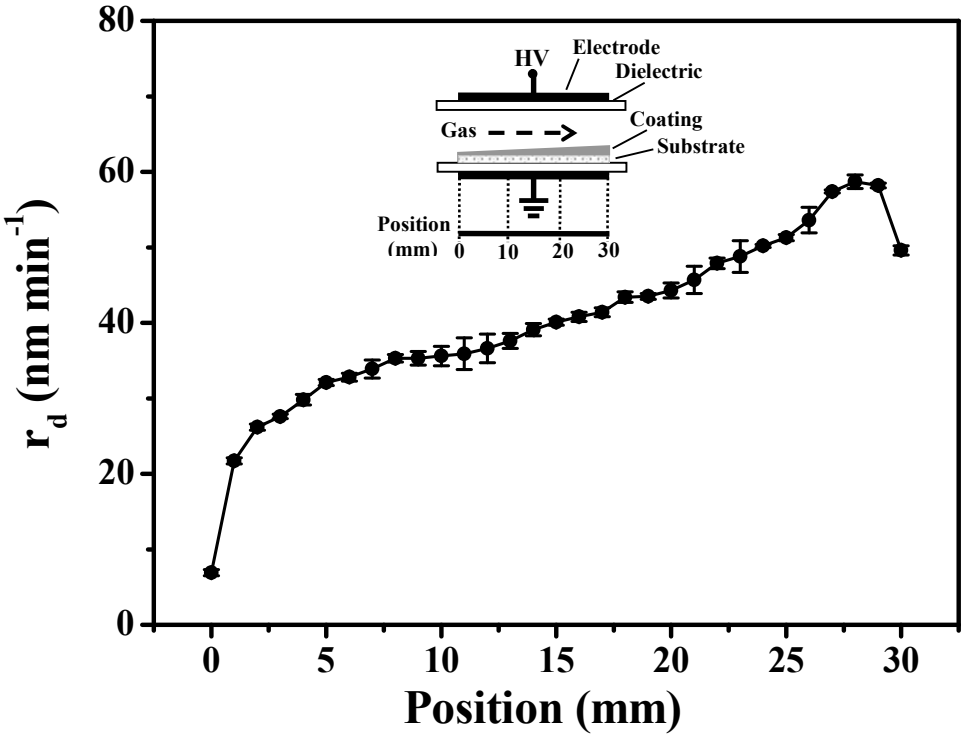
80
60
40
20
0
r_d (nm min^{-1})
0
5
10
15
20
25
30
Position (mm)
HV
Electrode
Dielectric
Coating
Gas
Substrate
Position (mm)
0
10
20
30

Figure 3

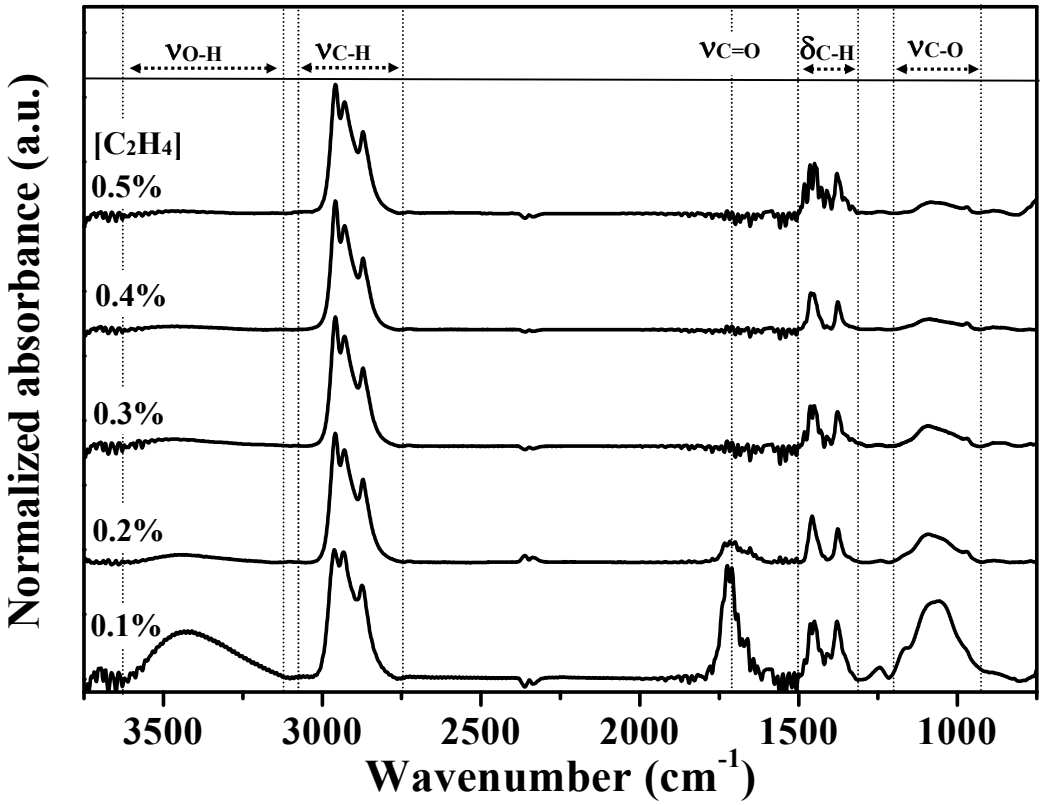
νO-H
νC-H
νC=O
δC-H
νC-O
[C2H4]
0.5%
0.4%
0.3%
0.2%
0.1%
Normalized absorbance (a.u.)
3500
3000
2500
2000
1500
1000
Wavenumber (cm-1)

Figure 4

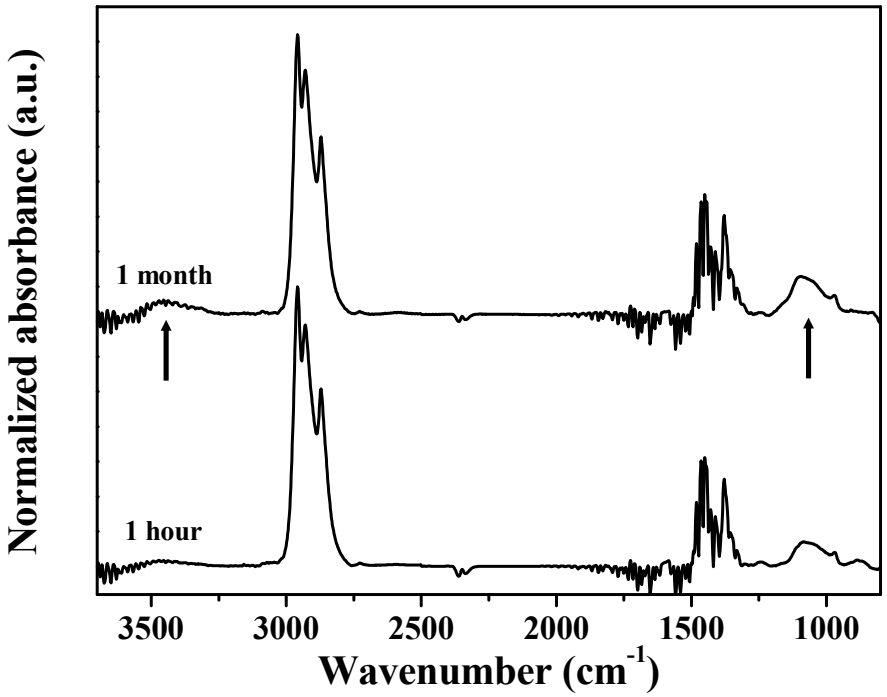
Normalized absorbance (a.u.)
1 month
1 hour
3500
3000
2500
2000
1500
1000
Wavenumber (cm-1)

Figure 5

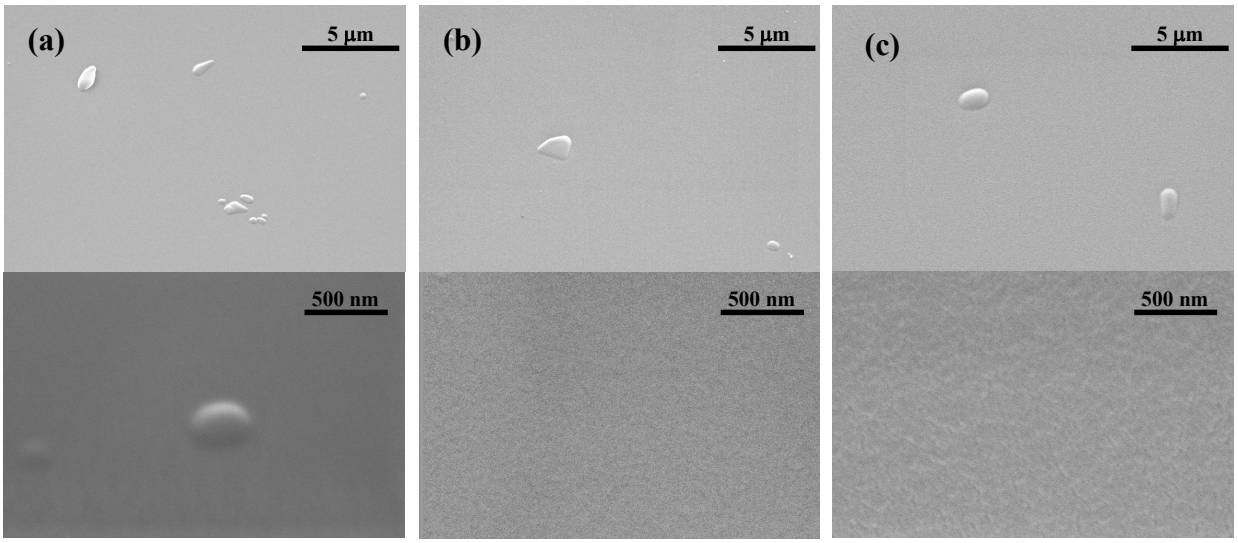

Figure 6

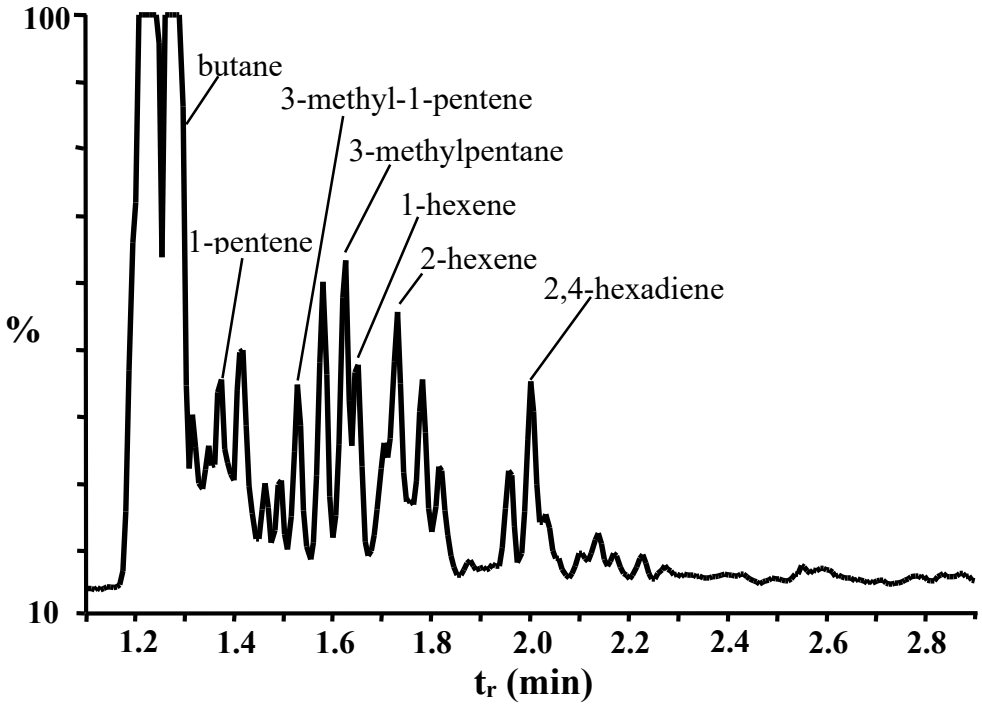
100
10
%
butane
3-methyl-1-pentene
3-methylpentane
1-hexene
1-pentene
2-hexene
2,4-hexadiene
1.2
1.4
1.6
1.8
2.0
2.2
2.4
2.6
2.8
t_r (min)

Figure 7